UC San Diego
UC San Diego Previously Published Works

Title

Understanding transmission and intervention for the COVID-19 pandemic in the United States

Permalink

https://escholarship.org/uc/item/19z8d98b

Authors

Li, Yixin
Zhang, Renyi
Zhao, Jiayun
et al.

Publication Date

2020-12-01

DOI

10.1016/j.scitotenv.2020.141560

Peer reviewed

Understanding transmission and intervention for the COVID-19 pandemic in the United States

Yixin Li [a], Renyi Zhang [a,b,*], Jiayun Zhao [a], Mario J. Molina [c,**]

[a] Department of Chemistry, Texas A&M University, College Station, TX 77843, USA
[b] Department of Atmospheric Sciences, Texas A&M University, College Station, TX 77843, USA
[c] Department of Chemistry and Biochemistry, University of California, San Diego, La Jolla, CA 92093, USA

HIGHLIGHTS

- Total infections and daily infections were analyzed in the top-fifteen infected U.S. states.
- All fifteen states exhibited initial sub-exponential and subsequent linear growth in total infections.
- Deviation from the linearity and curve flattening occurred after mandated face covering.
- Downward or slowing trends in daily cases occurred for most states after mandated face covering.

GRAPHICAL ABSTRACT
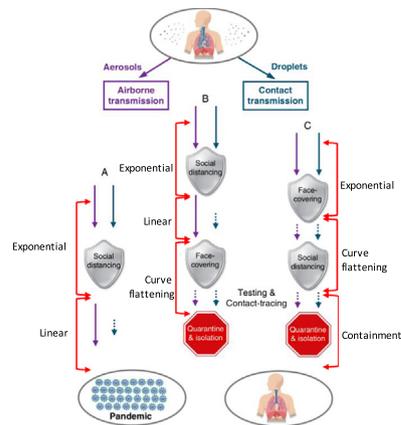
ARTICLE INFO

ABSTRACT

The outbreak of the novel coronavirus disease (COVID-19) severely threatens the public health worldwide, but the transmission mechanism and the effectiveness of mitigation measures remain uncertain. Here we assess the role of airborne transmission in spreading the disease and the effectiveness of face covering in preventing inter-human transmission for the top-fifteen infected U.S. states during March 1 and May 18, 2020. For all fifteen states, the curve of total confirmed infections exhibits an initial sub-exponential growth and a subsequent linear growth after implementing social distancing/stay-at-home orders. The linearity extends one to two months for the six states without mandated face covering and to the onset of mandated face covering for the other nine states with this measure, reflecting a dynamic equilibrium between first-order transmission kinetics and intervention. For the states with mandated face covering, significant deviation from this linearity and curve flattening occur after the onset of this measure for seven states, with exceptions for two states. Most states exhibit persistent upward trends in the daily new infections after social distancing/stay-at-home orders, while reversed downward or slowing trends occur for eight states after implementing mandated face covering. The inadequacy of social distancing and stay-at-home measures alone in preventing inter-human transmission is reflected by the continuous linear growth in the total infection curve after implementing these measures, which is mainly driven by airborne transmission. We estimate that the number of the total infections prevented by face covering reaches ~252,000 on May 18 in seven states, which is equivalent to ~17% of the total infections in the nation. We conclude that airborne transmission and face covering play the dominant role in spreading the disease and flattening the

* Correspondence to: Renyi Zhang, Department of Chemistry, Texas A&M University, College Station, TX 77843, USA.
** Corresponding author.
E-mail addresses: renyi-zhang@tamu.edu (R. Zhang), mjmolina@ucsd.edu (M.J. Molina).

total infection curve, respectively. Our findings provide policymakers and the public with compelling evidence that universal face covering, in conjunction with social distancing and hand hygiene, represents the maximal protection against inter-human transmission and the combination of these intervention measures with rapid and extensive testing as well as contact tracing is crucial in containing the COVID-19 pandemic.

1. Introduction

The COVID-19 outbreak has infected over 3.5 million people and caused over 139,000 fatalities on July 17, 2020 in the United States (US Centers for Disease Control and Prevention, 2020; World Health Organization, 2020). There exist two major routes for spreading the severe acute respiratory syndrome coronavirus 2 (SARS-CoV-2), namely contact and airborne transmissions (Kutter et al., 2018; Richard and Fouchier, 2016; Zhang et al., 2020). Viral shedding occurs primarily from breathing, talking, coughing, or sneezing by an infected person (Anfinrud et al., 2020; Leung et al., 2020; Stadnytskyi et al., 2020; Tang et al., 2013), producing respiratory particles of a variety of sizes: droplets ($> 5\,\mu m$) and aerosols ($< 5\,\mu m$). Contact transmission involves droplets deposited on a person (direct) or an object (indirect), and airborne transmission involves inhalation of virus-laden droplets or aerosols (Anfinrud et al., 2020; Leung et al., 2020; Stadnytskyi et al., 2020; Zhang et al., 2020). While transmission via direct or indirect contact occurs in a short distance, airborne transmission via aerosols takes place over an extended distance and time (Zhang et al., 2020). In addition, viral shedding for SARS-CoV-2 varies between symptomatic and asymptomatic carriers. A recent study demonstrated the highest viral load in the upper respiratory tract at the symptom onset, indicating substantial asymptomatic transmission for SARS-CoV-2 (He et al., 2020).

The mechanisms to spread the disease are not fully understood, particularly in terms of the relative contributions of the contact vs airborne transmission routes to the COVID-19 pandemic (Zhang et al., 2020). While contact transmission via respiratory droplets was initially considered as the dominant route in transmitting this virus (Chin et al., 2020; US Centers for Disease Control and Prevention, 2020; van Doremalen et al., 2020; World Health Organization, 2020), available epidemiological and experimental evidence has implicated airborne transmission of SARS-CoV-2 via respiratory aerosols as a probable route for the spreading of the disease (Liu et al., 2020; Morawska and Milton, 2020; Prather et al., 2020; van Doremalen et al., 2020). A recent analysis of the pandemic trends in Wuhan, Italy, and New York City revealed that the airborne transmission route dominated the spread of COVID-19 and face covering significantly shaped the outbreak trends in the three epicenters (Zhang et al., 2020). Currently, the subject on the transmission routes (i.e., contact versus airborne) for SARS-CoV-2 is highly debated among the research communities (Morawska and Milton, 2020), and the importance in airborne transmission likely differs between outdoor and indoor (especially community indoor) environments (Contini and Costabile, 2020; Zhang et al., 2020).

Various mitigation measures have been implemented in the U.S. to fight the COVID-19 pandemic, including social distancing, quarantine, isolation, stay-at-home orders, and face covering in public (World Health Organization, 2020; US Centers for Disease Control and Prevention, 2020; Zhang et al., 2020). Ideally, the mitigation measures are designated to intervene the virus transmission and to protect the public against infection. However, the effectiveness of mitigation measures remains uncertain, considerably hindering implementation of these measures to fight the COVID-19 pandemic. Evidence for prevention against transmission of SARS-CoV-2 by face covering has been provided in recent studies (Chu et al., 2020; Stutt et al., 2020). For example, a study on the association between masking and SARS-CoV-2 positivity among health care workers identified a significantly lower rate of SARS-CoV-2 positivity with universal masking in a health care system (Wang et al., 2020). Another work tracking 139 clients exposed to two symptomatic hair stylists with confirmed COVID-19 showed no symptomatic secondary cases when both stylists and the clients wore face masks (Hendrix et al., 2020).

SARS-CoV-2 is a novel virus with unprecedented transmission efficiency and interventions undertaken. While the appropriate methodology to model the transmission and intervention for a chaotic system such as COVID-19 has yet to be established, available empirical modeling framework for infectious disease dynamics requires scientific validation. Specifically, accurate representation of the large-scale behaviors is essential in modeling the COVID-19 pandemic. On the other hand, mismodeling occurs if the large-scale behaviors of the system are not accurately described, and overly emphasizing on details in the model only creates a false sense of confidence (Siegenfeld et al., 2020).

In this work, we assess the viral transmission and the effectiveness of mitigation measures in the U.S. during the period between March 1 and May 18, 2020. The trends of the cumulative confirmed infections and daily new confirmed cases in the fifteen states heavily plagued by COVID-19, which collectively account for about 78% of the total confirmed infections in the nation, are analyzed (see Table 1).

2. Methods

2.1. Statistical analysis

Statistical analysis was performed for the data of cumulative infections and daily new infections during each period using linear regression. The significance of the sub-exponential growth and subsequent linearity in the cumulative infections after stay-at-home orders for all fifteen states is reflected by the high correlation coefficients (R^2 ranging from 0.935 to 0.995 for the sub-exponential growth and from 0.986 to 0.999 for the linear growth). While the R^2 values in the daily new infections are low because of large fluctuations in the data, the slope of the regression reflects an upward (positive) or a downward (negative) trend in the data.

2.2. Estimation of the basic reproduction rate (R_0)

The cumulative confirmed cases (N) during the initial sub-exponential period (March 8 to April 12) is expressed as,

$$N = N_0 R_0^{t/\tau}$$

where N_0 is the initial confirmed cases, t is time in day, and τ is the serial interval for COVID-19, which is (3.96 ± 0.43) days (Du et al., 2020). The number of removed infections is small during the initial period. In the logarithmic plot (see Fig. 2), this equation is expressed as:

$$\log_{10}N = \log_{10}N_0 + \frac{\log_{10}R_0}{\tau}t$$

The basic reproduction rate (R_0) is calculated from,

$$R_0 = 10^{S \cdot \tau}$$

where S (d^{-1}) is the slope of the linear regression in Fig. 2.

Table 1
COVID-19 pandemic trend and projection of the difference in total infections by face covering in fifteen top-infected states of U.S.

	Daily confirmed cases				Total confirmed cases		
	Stay-at-home order[a]	S_1[b] (d^{-1})	Mandated face covering[a]	S_2[b] (d^{-1})	Sub-exp range	Linear range	Projected difference[c]
States without mandated face covering							
CA	3/19	24			3/8–4/2	4/3–5/18	
FL	4/3	−12			3/8–4/9	4/10–5/18	
GA	4/3	−4			3/8–4/5	4/6–5/18	
OH	3/24	7			3/8–4/2	4/3–5/18	
TX	4/2	11			3/8–4/10	4/11–5/18	
VA	3/30	15			3/8–4/11	4/12–5/18	
States with mandated face covering							
CT	3/24	34	4/21	−11	3/8–4/4	4/5–4/20	5835 (15%)
MA	3/24	31	5/6	−70	3/8–4/8	4/9–5/5	13,634 (16%)
MI	3/24	2.5	4/27	−13	3/8–3/27	3/28–4/26	8452 (16%)
NJ	3/22	127	4/14	−86	3/8–3/29	3/30–4/13	40,529 (27%)
NY	3/23	123	4/18	−181	3/8–3/27	3/28–4/17	168,884 (48%)
PA	4/1	−15	4/20	−21	3/8–4/2	4/2–4/19	13,086 (21%)
IL	3/22	50	5/1	−30	3/8–4/11	4/12–4/30	−12,113 (−12%)
LA	3/24	−18	5/1	−2	3/8–4/11	4/12–4/30	1122 (3.2%)
MD	3/31	23	4/18	12	3/8–4/2	4/3–4/17	−8546 (−20%)

[a] Orders that took effect after 5 pm are considered to start from the next day.

[b] S_1 denotes the slope of linear regression for the daily cases after stay-at-home order (for states without mandated face covering) or between stay-at-home order and mandated face covering, and S_2 denotes the slope of linear regression for the daily cases after mandated face covering

[c] The number of the total infections prevented by face covering is estimated from the difference on 18 May between the reported cases and the projected cases based on the linear regression using the data prior to implementing mandated face covering. The percentage is relative to the reported total cases on 18 May.

2.3. Definition of mandated face covering

The definitions of mandated face covering are summarized in Supplementary Table 1, with varying contents among the nine states with this measure. For example, New York required all citizens to wear a mask or a face covering in public and in situations where social distancing cannot be maintained. On the other hand, Louisiana required that all employees of a business who have contact with the public must wear a mask.

2.4. Projection of the difference in the total infections by face covering

Projection of the pandemic trend without face covering was performed by establishing the linear correlation between the total confirmed cases (y) and date (x) prior to implementing this measure for each state, with the onset date as $x = 0$. We considered the data ranging from 15 to 30 days prior to implementing mandated face covering, dependent on the regression to achieve the highest correlation coefficients. The derived regression was used for the projections, considering the high correlation coefficients for the data prior to the onset of mandated face covering.

2.5. Data sources

The COVID-19 confirmed cases for CA, FL, GA, OH, TX, VA, CT, MA, MI, NJ, NY, PA, IL, LA, and MD, respectively, were recorded from California Department of Public Health (https://www.cdph.ca.gov/Programs/CID/DCDC/pages/immunization/ncov2019.aspx#COVID-19%20by%20the%20Numbers), Florida Department of Health (https://floridahealthcovid19.gov/#latest-stats), Georgia Department of Public Health (https://dph.georgia.gov/covid-19-daily-status-report), Ohio Department of Health (https://coronavirus.ohio.gov/wps/portal/gov/covid-19/dashboards/overview), Texas Department of State Health Services (https://dshs.texas.gov/coronavirus/), Virginia Health Department (https://www.vdh.virginia.gov/coronavirus/), Connecticut government (https://data.ct.gov/stories/s/COVID-19-data/wa3g-tfvc/), Massachusetts Department of Public Health (https://www.mass.gov/info-details/covid-19-response-reporting), US CDC COVID Data Tracker (https://www.cdc.gov/covid-data-tracker/#trends), US CDC COVID Data Tracker (https://www.cdc.gov/covid-data-tracker/#trends), New York State Department of Health (https://covid19tracker.health.ny.gov/views/NYS-COVID19-Tracker/NYSDOHCOVID-19Tracker-Map?%3Aembed=yes&%3Atoolbar=no&%3Atabs=n), Pennsylvania Department of Health (https://www.health.pa.gov/topics/disease/coronavirus/Pages/Coronavirus.aspx), Illinois Department of Health (https://www.dph.illinois.gov/covid19/covid19-statistics), Louisiana Department of Health (http://ldh.la.gov/Coronavirus/), and Maryland Department of Health (https://coronavirus.maryland.gov/) daily at 6 pm ET.

3. Results

3.1. Two distinct growth stages in total confirmed infections

The initial outbreak in the fifteen U.S. states exhibits a sub-exponential growth in the number of total confirmed infections (Figs. 1 and 2), which is characteristic of the COVID-19 pandemic worldwide (Kucharski et al., 2020; Li et al., 2020; Maier and Brockmann, 2020; Zhang et al., 2020). This distinct sub-exponential increase lasted over a period of two to four weeks, i.e., from March 15 to April 12 (Table 1). The onset of the sub-exponential growth coincided with the issuing of the federal guidelines for social distancing on March 16 (US Centers for Disease Control and Prevention, 2020). In addition, all fifteen states implemented stay-at-home orders during the initial outbreak between March 19 and April 3, which also overlapped with the period of the sub-exponential growth.

Another key feature in the total infection curve is reflected by a remarkable linearity immediately following the initial sub-exponential growth (Figs. 1 and 3). The onsets of the linear growth of the total infections are between 0 and 20 days after the implementation of stay-at-home orders among the fifteen states. This linearity in the infection curve represents a dynamic equilibrium between transmission and mitigation measures. For the six states without implementing mandated face covering, the linearity extends one to two months until the end of our analysis period (May 18) (Figs. 1a–f and 3a–f). For example, the number of the total infections increases linearly from early April to May 18 for the states without mandated face covering, with the correlation coefficients ranging from 0.991 to 0.998. Nine states subsequently mandated face covering during the period of April 14 to May 6, and this implementation occurred 18 to 43 days later than those of the stay-at-home orders. For seven states with mandated face covering,
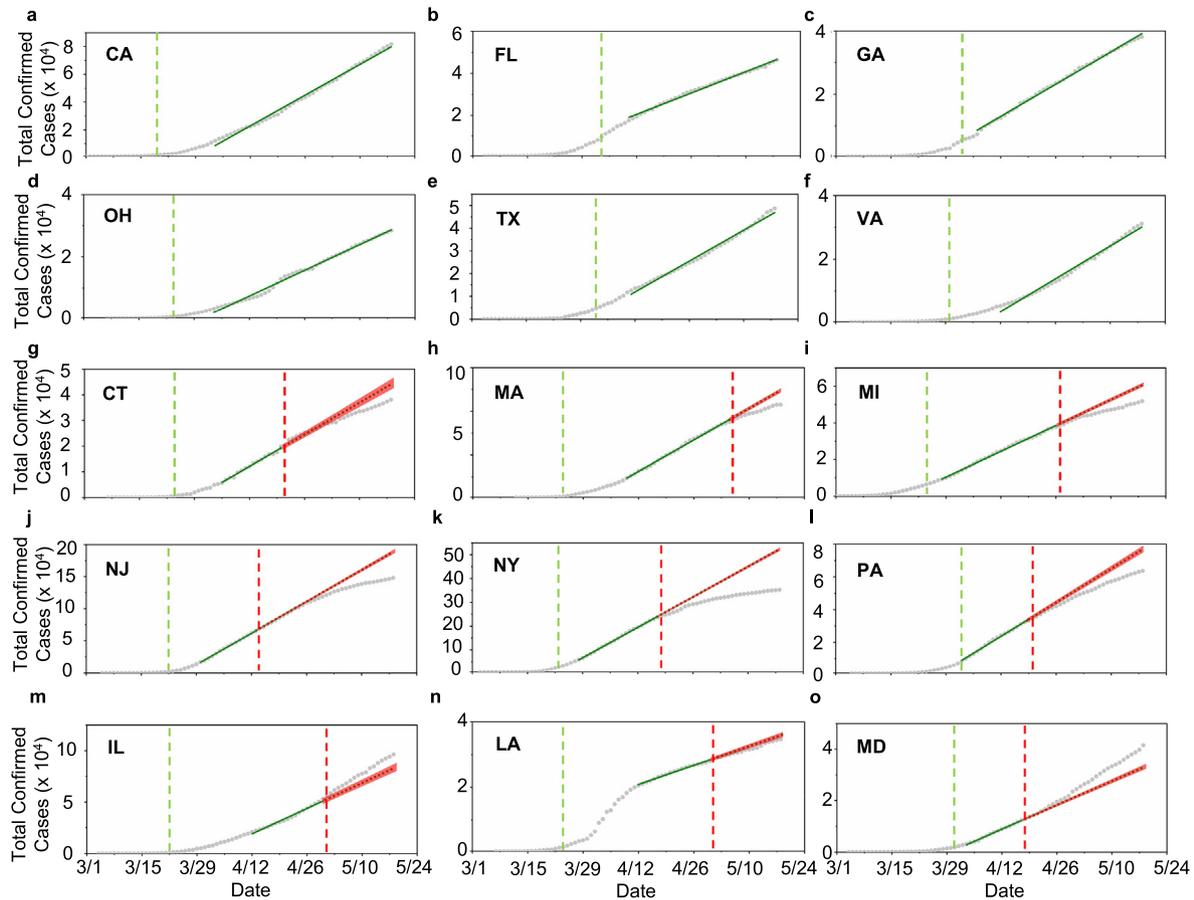
Fig. 1. Cumulative confirmed COVID-19 cases in the top-fifteen infected states of the U.S.; (a-f) For states without mandated face covering, a – California (CA), b – Florida (FL), c- Georgia (GA), d – Ohio (OH), e – Texas (TX), and f – Virginia (VA), (g-o) for states with mandated face covering, g – Connecticut (CT), h – Massachusetts (MA), i – Michigan (MI), j – New Jersey (NJ), k – New York (NY), l – Pennsylvania (PA), m – Illinois (IL), n – Louisiana (LA), and o – Maryland (MD). The vertical green and red dashed lines label the onsets for stay-at-home orders and mandated face covering, respectively. For comparison, guidelines for social distancing were issued by the federal government on March 16, 2020. The solid green line denotes linear regression through the data, and the dotted green line denotes projection of infections without face covering based on linear regression for the data prior to the onset of mandated face covering. The red shade (g-o) represents 95% confidence interval for the projection.

deviation from the linearity and curve flattening appear after the onset of mandated face covering (Fig. 1g–l, and n). Significant curve flattening is most evident in New York and New Jersey, occurring shortly after implementing this measure. Only two exceptions (Illinois and Maryland) show an unexpected upward trend in the number of total infections after mandated face covering (Fig. 1m and o).

3.2. Projection of the total infections prevented with face covering

We assessed the effects of face covering on the numbers of total infections by calculating the difference between projected and reported numbers in the total infections. This estimation is justifiable considering the high correlation coefficients (R^2 from 0.986 to 0.999) (Fig. 3g-o). The projection yields a range of total infections prevented by face covering for the nine states, with the two largest differences of ~168,000 (48%) in New York and ~41,000 (27%) in New Jersey (see Table 1). Overall, the total number of prevented infections with this measure is estimated to reach ~252,000 on May 18 in the seven states (Table 1), which is equivalent to ~17% of the total infections in the nation. For Illinois and Maryland, however, the projected values are lower than the reported numbers, by about 12% and 20%, respectively.

3.3. Trends in daily new cases

We analyzed the trend in the daily new cases by comparing the slopes of the linear regression during two periods of the pandemic,

which start after stay-at-home orders and mandated face covering. While the number in the daily new cases is highly fluctuating, the slopes of the linear regression (Table 1) provide an indication of the pandemic trend. The effects of face covering on curbing COVID-19 are also evident from the evolution in the daily new cases (Fig. 4). Comparison between states with and without mandated face covering unravels distinct trends. Eleven states exhibit upward trends in the daily new infections after the stay-at-home measures, as reflected by the positive slopes of the linear regression (Fig. 4 and Table 1). Four states defying this upward trend are Florida (Fig. 4b), Georgia (Fig. 4c), Pennsylvania (Fig. 4l), and Louisiana (Fig. 4n) with the largest spikes in the daily new cases between March 30 and April 8, which are likely attributed to spring-break mass gatherings prior to the stay-at-home orders. For California, Ohio, Texas, and Virginia without mandated face covering (Fig. 4a, d, e, and f), the increasing trend in the daily new cases persists throughout our analysis period. Six states with mandated face covering exhibit a reversed downward trend (i.e., from a positive to a negative slope for the linear regression), and two states exhibits a slowing trend (i.e., smaller slopes of the linear regression). Only Louisiana exhibits a downward trend after the stay-at-home and an increasing trend after face covering, which is explainable by spring-break mass gatherings.

4. Discussions

The distinct trends of the COVID-19 pandemic in the U.S. (Figs. 1–4) are explainable by the responsiveness of the mitigation measures
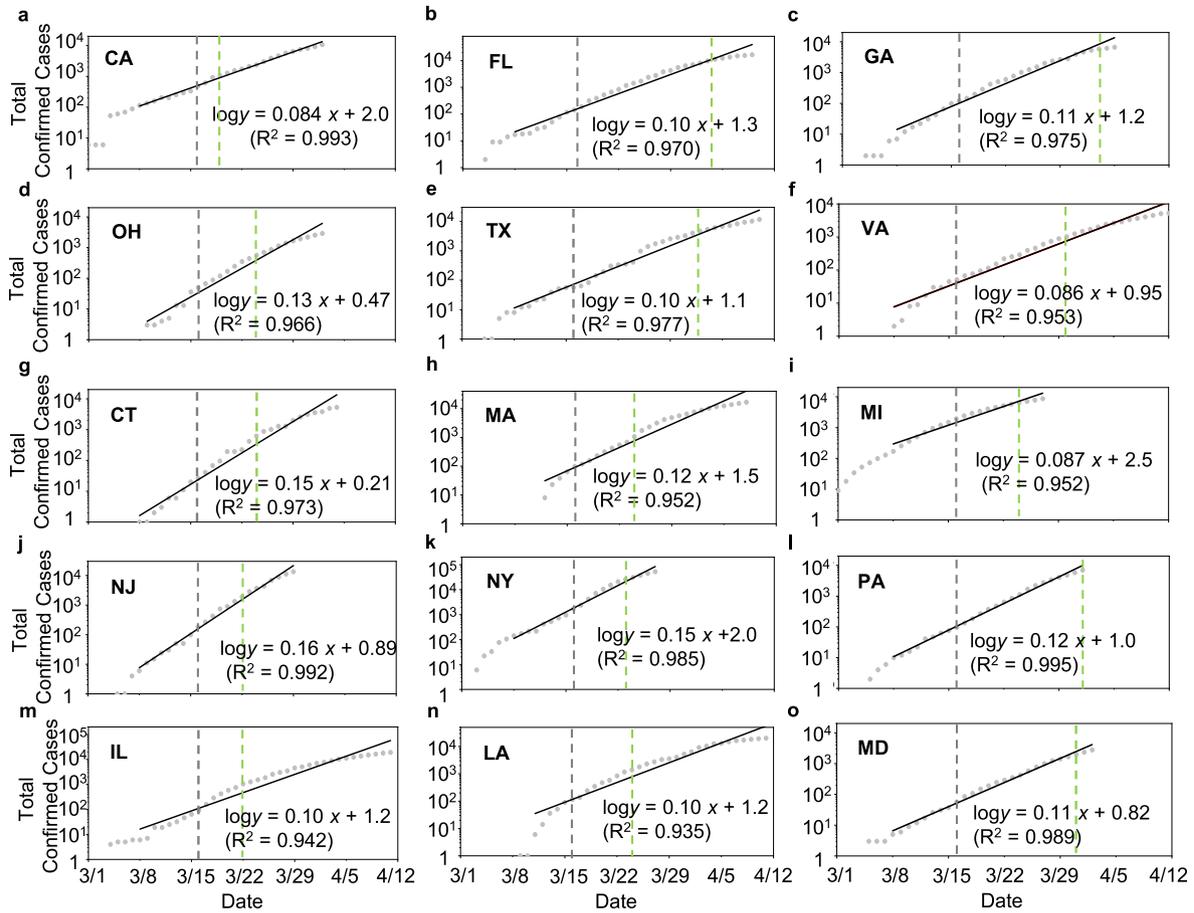
Fig. 2. Initial sub-exponential growth in the total infections; (a-f) For states without mandated face covering, a – CA, b –FL, c – GA, d – OH, e –TX, and f –VA, (g-o) for states with mandated face covering, g – CT, h – MA, i – MI, j – NJ, k – NY, l – PA, m – IL, n – LA, and o – MD. The vertical grey and green dashed lines label the beginning of social distancing and stay-at-home orders, respectively.

(Fig. 5). It has been suggested that a chaotic system such as COVID-19 is fundamentally unpredictable and understanding and modeling of the pandemics trends require accurate representation of the large-scale behaviors (Siegenfeld et al., 2020). The important first-order processes for COVID-19 include the transmission (contact versus airborne) for SARS-CoV-2, intervention (social distancing, stay-at-home, and mandated face-covering), and the interaction between transmission and intervention.

Social distancing, in conjunction with hand sanitizing, minimizes contact transmission but does not prevent airborne transmission. Compared to social distancing, the stay-at-home measure in principle limits both contact and airborne exposures. However, there exist many exceptions to the stay-at-home measure, including essential activities such as shopping for food and groceries and providing crucial services. These exceptions render airborne transmission as the most likely route to drive the disease spreading, when social distancing and hand-hygiene are still effective. In contrast, face covering prevents airborne transmission by blocking viral shedding and inhalation of virus-bearing aerosols as well as contact transmission by blocking viral shedding of droplets (Zhang et al., 2020). The combined face-covering, social distancing, and stay-at-home measures offer the maximal protections against contact and airborne exposures. Also, there exist plausible remnants of the mitigation measures, which arise from circumstances when the practices are not possible or are disobeyed and/or imperfection of the measures (Zhang et al., 2020). In addition, other second-order factors likely impact the pandemic trends, including the incubation period required from exposure to SARS-CoV-2 to development of symptoms, testing conducted, and uncertainties in data reporting. The incubation period

has been widely documented from epidemiological studies (Guan et al., 2020; Lauer et al., 2020; Li et al., 2020).

The changes in the total infection rate (defined as $R_N = \frac{dN}{dt}$, where N is the number of the total confirmed infections), is regulated by several forcing terms,

$$\frac{dR_N}{dt} = \sum_{i=1}^{2} T_i - \sum_{j=1}^{3} I_j + \sum_{k=1}^{n} O_k \tag{1}$$

where T_i is the transmission related to the contact ($i = 1$) and airborne ($i = 2$) routes, I_j is intervention ($j = 1$ for social distancing, $j = 2$ for stay-at-home order, and $j = 3$ for mandated face covering), and O_k denotes other second-order processes. The examples for O_k include remnants of intervention measures, citizens' actions prior to mandated measures, and variations in testing and data reporting.

For the initial sub-exponential period in the absence of intervention and secondary forcing, the change in the infection rate is expressed as,

$$\frac{dR_N}{dt} = \sum_{i=1}^{2} T_i > 0 \tag{2}$$

The Eq. (2) is conventionally transformed to the following form, in which the infection rate is proportional to the number of the total confirmed cases,

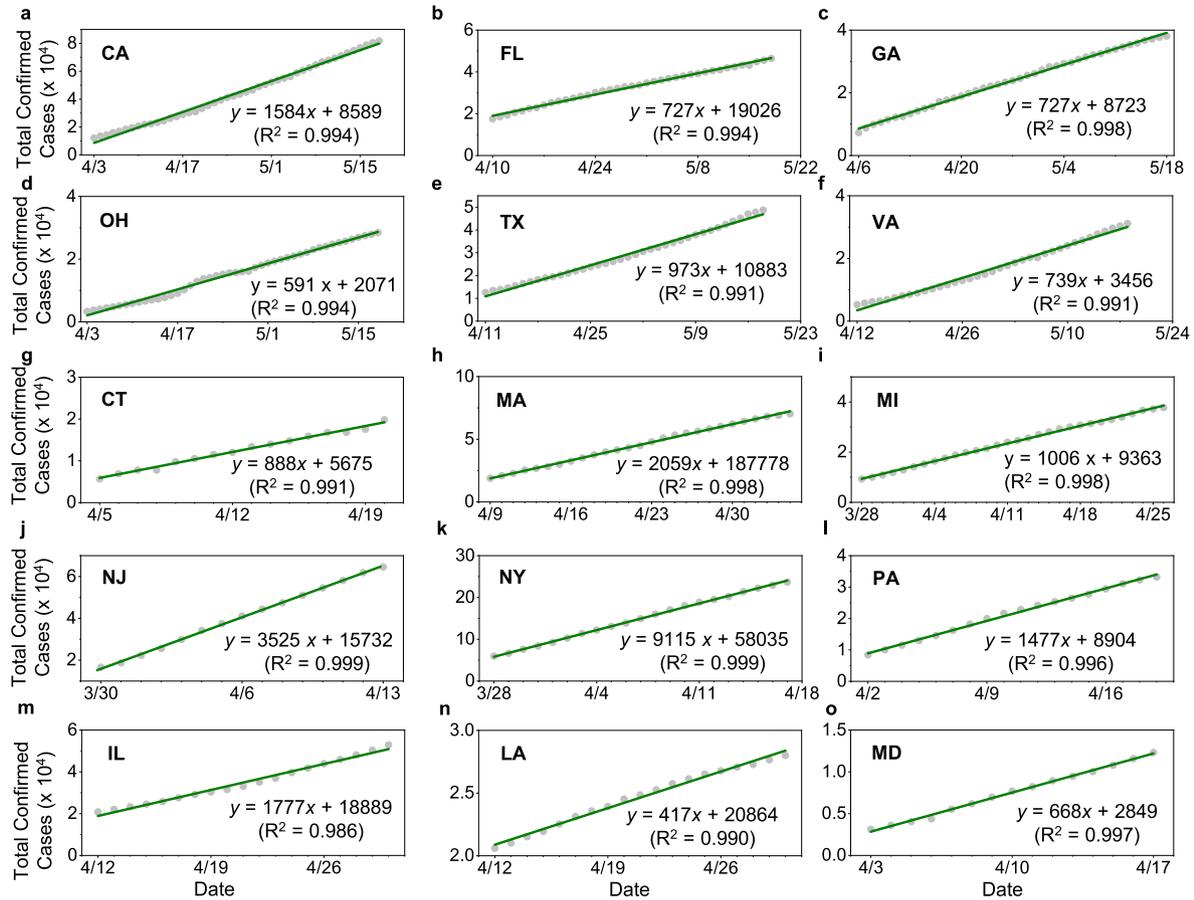$$\frac{dN}{dt} = N\beta \text{ or } \frac{dR_N}{dt} = N\beta^2 \tag{3}$$

Fig. 3. Linear increase in the total infections following the initial sub-exponential growth; (a-f) For states without mandated face covering, a – CA, b –FL, c – GA, d – OH, e –TX, and f –VA, (g-o) for states with mandated face covering, g – CT, h – MA, i – MI, j – NJ, k – NY, l – PA, m – IL, n – LA, and o – MD. The dates cover the range from the end of the sub-exponential growth period (in Fig. 2) to 18 May for a-f or to the onset of mandated face covering for g-o.

where β is the estimated number of people that an infected person infects per day ($\beta = \frac{\ln R_0}{\tau}$). For the fifteen states, the slope of the linear regression (S) in Fig. 2 is equal to 0.11 ± 0.02 d^{-1}. The average value of R_0 is estimated to be 2.8 ± 0.8, and the average value of β is calculated to be 0.26 ± 0.10 d^{-1} for the initial sub-exponential period, consistent with other previous studies (Kucharski et al., 2020; Li et al., 2020; Maier and Brockmann, 2020).

The containment of the initial sub-exponential growth and subsequent conversion to the linear growth in the total infections during the early outbreak are attributable to social distancing and stay-at-home measures, because of reduced contact transmission (T_1). In addition, the duration of two to five weeks for the sub-exponential growth is relevant to the timing for implementation of social distancing and stay-at-home measures, the incubation period required from exposure to SARS-CoV-2 to development of symptoms, testing conducted, and data reporting for the COVID-19 confirmed cases.

Although the combined social distancing (in conjunction with hand sanitizing) and stay-at-home measures reduce contact transmission (T_1), they are ineffective in protecting against airborne transmission (T_2), as reflected by the linear growth in the total infection curve after implementing social distancing/stay-at-home measures (Figs. 1 and 3). Specifically, the exceptions to the stay-at-home measure, such as shopping for food and groceries and providing crucial services, render airborne transmission as the only viable route for the disease spreading, when social distancing and hand-hygiene are exercised. Hence, the linear growth in the total infection curve is primarily driven by airborne transmission (T_2). The linearity in the total infection curve after social

distancing/stay-at-home measures is regulated by the dynamic equilibrium between the first-order airborne transmission and intervention as well as the combined second-order effects, including face covering prior to and/or without the mandated measure. The change in the infection rate after implementation of social distancing/stay-at-home orders is $\frac{dR_N}{dt} = 0$, corresponding to an overall canceling effect among the forcing terms. After implementing the social distancing/stay-at-home measures, airborne transmission (T_2) remains as the first-order process, while contact transmission (T_1) is reduced to a second-order process (remnant).

Recent measurements have identified SARS-CoV-2 RNA on aerosols in Wuhan's hospitals (Liu et al., 2020) and in Northern Italy (Setti et al., 2020), indicating the likelihood for the airborne route. The high efficiency of airborne transmission of SARS-CoV-2 is explained by several factors. Human inhalation of respiratory aerosols leads to direct and deep deposition into the respiratory tract (Rychlik et al., 2019; Wu et al., 2019). Also, virus-laden aerosols have great mobility and sufficiently long surviving-time for dispersion in air (Liu et al., 2020; Rychlik et al., 2019; Zhang et al., 2015). In addition, nascent micron-size aerosols produced from viral shedding of asymptomatic carriers have the potential of containing many viruses (He et al., 2020; Zhang et al., 2020). Furthermore, airborne transmission likely occurs more efficiently indoors than outdoors, because of less ventilation and dilution of respiratory aerosols indoors (Zhang et al., 2020).

The subsequent implementation of mandated face covering disrupts the dynamic equilibrium between airborne transmission and social distancing/stay-at-home measures. The effects of face covering on
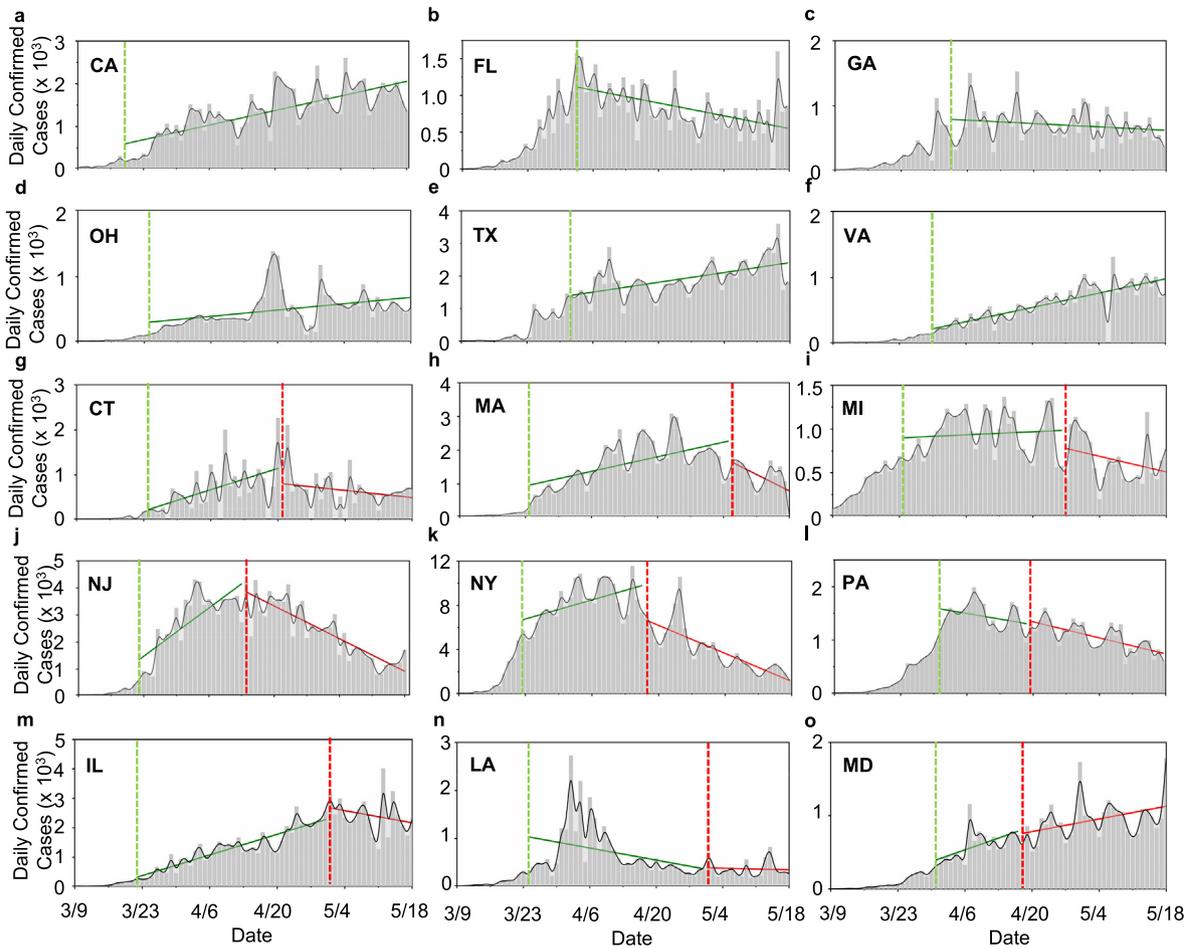
Fig. 4. Trends in the daily new infections; (a-f) For states without mandated face covering, a – CA, b –FL, c – GA, d – OH, e –TX, and f –VA, (g-o) for states with mandated face covering, g – CT, h – MA, i – MI, j – NJ, k – NY, l – PA, m – IL, n – LA, and o – MD. The vertical green and red dashed lines label the onsets for stay-at-home orders and mandated face covering, respectively, and the solid green and red lines represent linear regression through the data.

reducing both contact and airborne transmissions result in an overall negative forcing term, i.e., $\frac{dR_N}{dt} < 0$, explaining the departure from the linearity and curve flattening in most states with mandated face covering (Fig. 1). Hence, the combined social distancing/stay-at-home measures and face covering provide additional prevention against airborne

transmission (Fig. 5). The onset of the curve flattening is relevant to the timing of implementation of mandated face covering, the incubation period, testing conducted, and data reporting for COVID-19. In addition, the second-order effect of face covering among citizens prior to the mandated measure also exerts an impact on curve flattening, likely
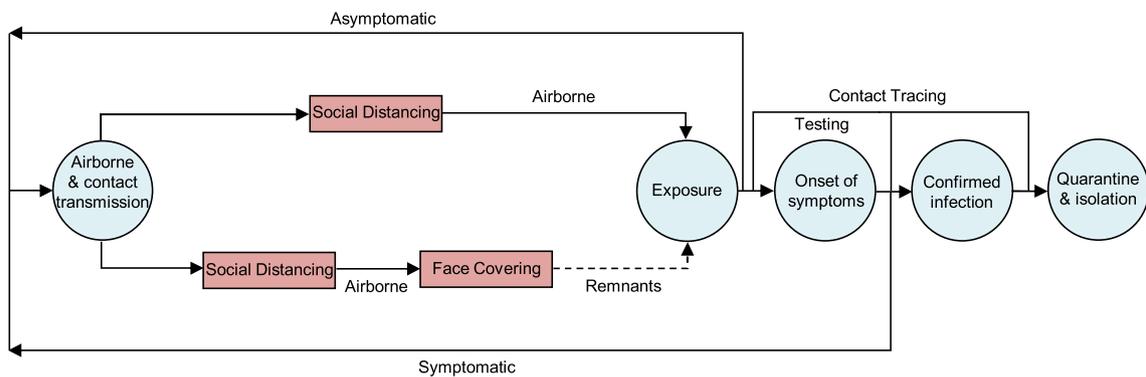

Fig. 5. Transmission and intervention of COVID-19 in the U.S.; The boxes denote mitigation measures, and the circles depict the disease evolution. Transmission starts from viral shedding by asymptomatic and symptomatic carriers and occurs via the contact and airborne routes. Social distancing, in conjunction with hand sanitizing, minimizes contact transmission, rendering airborne transmission as the most likely route. The remnants after the combined social distancing and face covering (dashed line) account for possible virus transmission due to circumstances when excising the measure is not possible or the measure is disobeyed and/or due to imperfection of the measure. The combined face covering and social distancing measures with rapid and extensive testing as well as contact tracing is key to curbing the COVID-19 pandemic.

explaining the earlier onset in New York. Advice of using face masks was made on April 3 by the U.S. Centers for Disease Control and Prevention (CDC) and on April 6 by the World Health Organization (WHO) (US Centers for Disease Control and Prevention, 2020; World Health Organization, 2020). Those various factors jointly explain the differences in the onsets of the curve flattening among the seven states. The continuous increase in the total confirmed cases after face covering is attributed to the remnants of the mitigation measures as well as inadequate testing, lacking contact tracing, and asymptomatic transmission. Also, the timing and sequence in implementing the mitigation measures exert distinct outcomes on the pandemic (Zhang et al., 2020). The implementation of mandated face covering was delayed by 18–43 days than those of the stay-at-home orders, allowing an extended period for uninterrupted airborne transmission to spread the disease.

The uncertainty in assessing the effectiveness of face covering is relevant to several factors, including the remnants of this measure and other second-order effects. For example, the curve flattening in the total infections is most pronounced in New York and New Jersey, likely due to strict enforcement of this measure after both emerging as the most infected states of COVID-19 in the nation. In addition, variations in the number of COVID-19 testing conducted, data reporting, and mass gatherings also contribute to the anomalies of the pandemic trends, such as the large spikes in Florida, Georgia, Pennsylvania, and Louisiana in early April (Fig. 4). Also, the upward trend in Illinois after mandated face covering is likely related to reported mass gathering of house parties (with more than 1000 people) on April 25 and protests around May 1. For Maryland, the upward trend is likely related to reported gathering of protests demanding reopening the economy on April 18 as well as obtaining 500,000 coronavirus tests from South Korea on April 20.

Under loosened mitigation measures, both contact and airborne transmission routes are re-invigorated, and the reduced mitigation measures result in an overall positive effect among the forcing terms. Hence, the change in the infection rate is $\frac{dR_N}{dt} > 0$ under relaxed social distancing, stay-at-home, and face-covering measures, leading to an upward trend. This scenario likely corresponds to those in Illinois and Maryland after the onset of mandated face covering and to those in Texas and Florida after reopening the economy on May 1 and May 4, respectively. Large spikes in the daily new cases are evident after reopening for both Texas and Florida (Fig. 4b and e).

Notably, the uncertainties of face covering in protecting inter-human transmission, which have been emphasized by the WHO (World Health Organization, 2020), have resulted in intensive debates on wearing face masks to prevent inter-human transmission during the pandemic (Howard et al., 2020; Chu et al., 2020) and inconsistent recommendations by U.S. CDC and WHO (US Centers for Disease Control and Prevention, 2020; World Health Organization, 2020). Evidence for the effectiveness of face covering has been recently recognized, showing reduced emissions of respiratory droplets and aerosols when worn by infected individuals (Cheng et al., 2020) and prevented inter-human transmission (Hendrix et al., 2020; Wang et al., 2020).

The extent of the COVID-19 pandemic is significantly larger than those of other recent outbreaks caused by respiratory viruses, including the 2002/2003 SARS-CoV-1 and the Middle East Respiratory Syndrome coronavirus (MERS-CoV) (Assiri et al., 2013; Haagmans et al., 2014; Lloyd-Smith et al., 2005; Peiris et al., 2003). On the other hand, available experimental evidence indicated comparable survival and stability of SARS-CoV-2 on surfaces and aerosols to those of the analogous coronavirus SARS-CoV-1 and MERS-CoV (Chin et al., 2020; Pyankov et al., 2018; van Doremalen et al., 2020). The severity and epidemiological characteristics for the COVID-19 pandemic are likely attributed to the unique viral shedding for SARS-CoV-2, particularly from asymptomatic transmission (Liu et al., 2020).

There exist many first-order (T_i and I_j) and second-order (O_k) processes that regulate the transmission and intervention, posing

enormous challenges for modeling the pandemic trends (Siegenfeld et al., 2020; Zhang et al., 2020). While detailed modeling for the COVID-19 pandemic trend is beyond the scope of our work, the framework developed in our study provides the guidance to understand and model the COVID-19 pandemic, by emphasizing the first-order processes for viral transmission mechanisms, interventions, and their interactions. Specifically, our approach captures and represents the essential first-order processes, i.e., the transmission routes of SARS-CoV-2 (contact vs airborne transmission), the interventions (social distancing/stay-at-home and mandated face-covering), and the interaction between transmission routes and interventions. Furthermore, our work explains the pandemic trend at multiple locations and provides insight to development of intervention policies to constrain the spread of COVID-19 pandemic (Supplementary Fig. 1).

More broadly, this topic is relevant to bioaerosols – a research field that has a long-lasting history (Fröhlich-Nowoisky et al., 2016; Brooks et al., 2019), when mold spores were detected in air by Charles Darwin in 1833. A variety of pathogenic microorganisms exists in air, including bacteria, fungi, viruses, and their derivatives. Several facts likely regulate the physicochemical properties of bioaerosols that determine their fate, transformation, and transport in open and confined spaces, including growth by condensation/partitioning/multiphase reactions, coagulation, and removal by wet and dry deposition (An et al., 2019). Also, airborne viral transmission is dependent on air conditions, i.e., temperature, humidity, and solar radiation, which vary considerably between open and confined spaces. While the atmospheric conditions are significantly different during the period of March 1 to May 18 and among the fifteen states, indoor conditions are typically less variable (Wallace et al., 2002).

5. Summary and conclusions

In this study, we analyzed the cumulative confirmed infections and daily new infections from March 1 to May 18, 2020 for the top-fifteen states heavily plagued in the U.S. During this period, unique intervention measures, such as social distancing, stay-at-home, and mandated face covering, were undertaken, and our results illustrate that these measures have contributed to the distinct trends in the total infections as well as the daily new infections.

Our analysis reveals that there exist an initial sub-exponential (an overall positive forcing term in eq. 1) and a subsequent linear growth in the total confirmed infections for all fifteen states. The linearity in the total confirmed infections emerges between 0 and 20 days after implementing stay-at-home orders and extends one to two months for the six states without mandated face covering or to the onset of mandated face covering orders for nine states with this measure. This remarkable linearity reflects a dynamic equilibrium among the first-order forcing terms, i.e., transmission, intervention, and the interaction between transmission and intervention as well as combined (addition or canceling) second-order effects (eq. 1). Deviation from this linearity and curve flattening occur after the onset of mandated face covering for seven states. For the daily new confirmed cases, eleven states exhibit persistent upward trends after social distancing/stay-at-home orders, while eight states show reversed downward or slowing trends after implementing mandated face covering. We estimate that the number of the total infections prevented by face covering reaches ~252,000 on May 18 in seven states, which is equivalent to ~17% of the total infections in the nation.

The inadequacy of social distancing and stay-at-home measures alone in preventing inter-human transmission is illustrated by the continuous linear growth in the total infection curve after implementing these measures (Figs.1 and 3). In particular, this linearity persists one to two months for the six states without mandated face covering. The combined social distancing, hand sanitizing, and stay-at-home measures reduce contact transmission, but are ineffective in protecting airborne transmission without face covering. The linear growth in the

total infection curve after implementing the social distancing/stay-at-home measures is mainly driven by airborne transmission. The dominant role of airborne transmission in spreading the COVID-19 pandemic is jointly explainable by several facts relevant to virus-laden aerosols, i.e., direct and deep deposition into the respiratory tract by inhalation, great mobility and sufficiently long surviving-time for dispersion in air, and high viral contents from asymptomatic carriers (Zhang et al., 2020). The subsequent implementation of mandated face covering disrupts the dynamic equilibrium between airborne transmission and social distancing/stay-at-home measures. The addition of face covering results in an overall negative forcing term (Eq. (1)), leading to the departure from the linearity and curve flattening in most states with mandated face covering. Under relaxed social distancing, stay-at-home, and face-covering measures, the overall effect among the forcing terms becomes positive, leading to an upward pandemic trend after reopening the economy. Future studies are necessary to assess the effects of relaxed mitigation measures on the second wave of the pandemic in the U.S.

In summary, our results corroborate the importance of airborne transmission in spreading the disease and face covering in preventing inter-human transmission (Zhang et al., 2020). As only one third of the U.S. states implemented mandated face covering by May 18 (Supplementary Fig. 2), our findings highlight the necessity of face covering in curbing the spread of the disease. In particular, universal face covering, in conjunction with social distancing and hand hygiene, provides the maximal protection against inter-human transmission and the combination of these intervention measures with rapid and extensive testing as well as contact tracing represents the key in containing the COVID-19 pandemic (Fig. 5).

CRediT authorship contribution statement

Yixin Li: Investigation, Validation, Writing - review & editing. **Renyi Zhang:** Conceptualization, Investigation, Validation, Writing - original draft, Writing - review & editing. **Jiayun Zhao:** Investigation, Validation. **Mario J. Molina:** Investigation, Validation, Writing - review & editing.

Declaration of competing interest

The authors declare that they have no known competing financial interests or personal relationships that could have appeared to influence the work reported in this paper.

Data availability

The authors declare that all relevant data supporting the finding of this study are available within the paper and its supplementary information files. All data are available from the corresponding author on reasonable request. Source data are provided with this paper.

Appendix A. Supplementary data

Supplementary data to this article can be found online at https://doi.org/10.1016/j.scitotenv.2020.141560.

References

An, Z., Huang, R.J., Zhang, R., Tie, X., Li, G., Cao, J., Zhou, Z., Shi, Z., Han, Y., Gu, Z., Ji, Y., 2019. Severe haze in Northern China: A synergy of anthropogenic emissions and atmospheric processes. Proc. Natl. Acad. Sci. U. S. A. 116, 8657–8666. https://doi.org/10.1073/pnas.1900125116.

Anfinrud, P., Bax, C.E., Bax, A., 2020. Visualizing speech-generated oral fluid droplets with laser light scattering. N. Engl. J. Med. 382, 2061–2063. https://doi.org/10.1056/NEJMc2007800.

Assiri, A., McGeer, A., Perl, T.M., Price, C.S., Al Rabeeah, A.A., Cummings, D.A.T., Alabdullatif, Z.N., Assad, M., Almulhim, A., Makhdoom, H., Madani, H., Alhakeem, R., Al-Tawfiq, J.A., Cotten, M., Watson, S.J., Kellam, P., Zumla, A.I., Memish, Z.A., 2013. Hospital outbreak of Middle East respiratory syndrome coronavirus. N. Engl. J. Med. 369, 407–416. https://doi.org/10.1056/NEJMoa1306742.

Brooks, S.D., Jickells, T.D., Liss, P.S., Thornton, D.C.O., Zhang, R., 2019. Biogeochemical coupling between ocean and atmosphere—a tribute to the lifetime contribution of Robert A. Duce. J. Atmos. Sci. 76, 3289–3298.

Cheng, K.K., Lam, T.H., Leung, C.C., 2020. Wearing face masks in the community during the COVID-19 pandemic: altruism and solidarity. Lancet Published online April 16, 2020. https://doi.org/10.1016/S0140-6736(20)30918-1.

Chin, A.W.H., Chu, J.T.S., Perera, M.R.A., Hui, K.P.Y., Yen, H.-L., Chan, M.C.W., Peiris, M., Poon, L.L.M., 2020. Stability of SARS-CoV-2 in different environmental conditions. Lancet 1, E10. https://doi.org/10.1016/S2666-5247(20)30003-3.

Chu, D.K., Akl, E.A., Duda, S., Solo, K., Yaacoub, S., Schünemann, H.J., Chu, D.K., Akl, E.A., El-harakeh, A., Bognanni, A., Lotfi, T., Loeb, M., Hajizadeh, A., Bak, A., Izcovich, A., Cuello-Garcia, C.A., Chen, C., Harris, D.J., Borowiack, E., Chamseddine, F., Schünemann, F., Morgano, G.P., Muti Schünemann, G.E.U., Chen, G., Zhao, H., Neumann, I., Chan, J., Khabsa, J., Hneiny, L., Harrison, L., Smith, M., Rizk, N., Giorgi Rossi, P., AbiHanna, P., El-khoury, R., Stalteri, R., Baldeh, T., Piggott, T., Zhang, Y., Saad, Z., Khamis, A., Reinap, M., Duda, S., Solo, K., Yaacoub, S., Schünemann, H.J., 2020. Physical distancing, face masks, and eye protection to prevent person-to-person transmission of SARS-CoV-2 and COVID-19: a systematic review and meta-analysis. Lancet 395, 1973–1987. https://doi.org/10.1016/s0140-6736(20)31142-9.

Contini, D., Costabile, F., 2020. Does Air Pollution Influence COVID-19 Outbreaks? Atmosphere 11, 377. https://doi.org/10.3390/atmos11040377.

van Doremalen, N., Morris, D.H., Holbrook, M.G., Gamble, A., Williamson, B.N., Tamin, A., Lloyd-Smith, J.O., de Wit, E., 2020. Aerosol and surface stability of SARS-CoV-2 as compared with SARS-CoV-1. N. Engl. J. Med. 382, 1564–1567. https://doi.org/10.1056/NEJMc2004973.

Du, Z., Xu, X., Wu, Y., Wang, L., Cowling, B.J., Meyers, L., 2020. Serial interval of COVID-19 among publicly reported confirmed cases. Emerg. Infect. Dis. 26 (6), 1341–1343. https://doi.org/10.3201/eid2606.200357.

Fröhlich-Nowoisky, J., et al., 2016. Bioaerosols in the earth system: climate, health, and ecosystem interactions. Atmos. Res. 182, 346–376.

Guan, W., Ni, Z., Hu, Yu Liang, W., Ou, C., He, J., Liu, L., Shan, H., Lei, C., Hui, D.S.C., Du, B., Li, L., Zeng, G., Yuen, K.-Y., Chen, R., Tang, C., Wang, T., Chen, P., Xiang, J., Li, S., Wang, Jin-lin, Liang, Z., Peng, Y., Wei, L., Liu, Y., Hu, Ya-hua, Peng, P., Wang, Jian-ming, Liu, J., Chen, Z., Li, G., Zheng, Z., Qiu, S., Luo, J., Ye, C., Zhu, S., Zhong, N., 2020. Clinical characteristics of coronavirus disease 2019 in China. N. Engl. J. Med. 382, 1708–1720. https://doi.org/10.1056/NEJMoa2002032.

Haagmans, B.L., Al Dhahiry, S.H.S., Reusken, C.B.E.M., Raj, V.S., Galiano, M., Myers, R., Godeke, G.-J., Jonges, M., Farag, E., Diab, A., Ghobashy, H., Alhajri, F., Al-Thani, M., Al-Marri, S.A., Al Romaihi, H.E., Al Khal, A., Bermingham, A., Osterhaus, A.D.M.E., AlHajri, M.M., Koopmans, M.P.G., 2014. Middle East respiratory syndrome coronavirus in dromedary camels: an outbreak investigation. Lancet Infect. Dis. 14, 140–145. https://doi.org/10.1016/S1473-3099(13)70690-X.

He, X., Lau, E., Wu, P., Deng, X., Wang, J., Hao, X., Lau, Y.C., Wong, J.Y., Guan, Y., Tan, X., Mo, X., Chen, Y., Liao, B., Chen, W., Hu, F., Zhang, Q., Zhong, M., Wu, Y., Zhao, L., Zhang, F., Cowling, B.J., Li, F., Leung, G.M., 2020. Temporal dynamics in viral shedding and transmissibility of COVID-19. Nat. Med. 26 (5), 672–675. https://doi.org/10.1038/s41591-020-0869-5.

Hendrix, M.J., Walde, C., Findley, K., Trotman, R., 2020. Absence of apparent transmission of SARS-CoV-2 from two stylists after exposure at a hair salon with a universal face covering policy — Springfield, Missouri, May 2020. MMWR Morb. Mortal. Wkly Rep. 69, 930–932. https://doi.org/10.15585/mmwr.mm6928e2external icon.

Howard, J., Huang, A., Li, Z., Tufekci, Z., Zdimal, V., van der Westhuizen, H., von Delft, A., Price, A., Fridman, L., Tang, L., Tang, V., Watson, G.L., Bax, C.E., Shaikh, R., Questier, F.; Hernandez, D., Chu, L.F., Ramirez, C.M., Rimoin, A.W., 2020. Face Masks Against COVID-19: An Evidence Review. 2020040203. doi:10.20944/preprints202004.0203.v2. Accessed May 18, 2020.

Kucharski, A.J., Russell, T.W., Diamond, C., Liu, Y., Edmunds, J., Funk, S., Eggo, R.M., Sun, F., Jit, M., Munday, J.D., Davies, N., Gimma, A., van Zandvoort, K., Gibbs, H., Hellewell, J., Jarvis, C.I., Clifford, S., Quilty, B.J., Bosse, N.I., Abbott, S., Klepac, P., Flasche, S., 2020. Early dynamics of transmission and control of COVID-19: a mathematical modelling study. Lancet Infect. Dis. 20, 553–558. https://doi.org/10.1016/S1473-3099(20)30144-4.

Kutter, J.S., Spronken, M.I., Fraaij, P.L., Fouchier, R.A., Herfst, S., 2018. Transmission routes of respiratory viruses among humans. Curr. Opin. Virol. 28, 142–151. https://doi.org/10.1016/j.coviro.2018.01.001.

Lauer, S.A., Grantz, K.H., Bi, Q., Jones, F.K., Zheng, Q., Meredith, H.R., Azman, A.S., Reich, N.G., Lessler, J., 2020. The incubation period of coronavirus disease 2019 (COVID-19) from publicly reported confirmed cases: estimation and application. Ann. Intern. Med. 172, 577–582. https://doi.org/10.7326/M20-0504.

Leung, N.H.L., Chu, D.K.W., Shiu, E.Y.C., Chan, K.-H., McDevitt, J.J., Hau, B.J.P., Yen, H.-L., Li, Y., Ip, D.K.M., Peiris, J.S.M., Seto, W.-H., Leung, G.M., Milton, D.K., Cowling, B.J., 2020. Respiratory virus shedding in exhaled breath and efficacy of face masks. Nat. Med. 26, 676–680. https://doi.org/10.1038/s41591-020-0843-2.

Li, Q., Guan, X., Wu, P., Wang, X., Zhou, L., Tong, Y., Ren, R., Leung, K.S.M., Lau, E.H.Y., Wong, J.Y., Xing, X., Xiang, N., Wu, Y., Li, C., Chen, Q., Li, D., Liu, T., Zhao, J., Liu, M., Tu, W., Chen, C., Jin, L., Yang, R., Wang, Q., Zhou, S., Wang, R., Liu, H., Luo, Y., Liu, Y., Shao, G., Li, H., Tao, Z., Yang, Y., Deng, Z., Liu, B., Ma, Z., Zhang, Y., Shi, G., Lam, T.T.Y., Wu, J.T., Gao, G.F., Cowling, B.J., Yang, B., Leung, G.M., Feng, Z., 2020. Early transmission

dynamics in Wuhan, China, of novel coronavirus–infected pneumonia. N. Engl. J. Med. 382, 1199–1207. https://doi.org/10.1056/NEJMoa2001316.

Liu, Y., Ning, Z., Chen, Y., Guo, M., Liu, Yingle, Gali, N.K., Sun, L., Duan, Y., Cai, J., Westerdahl, D., Liu, X., Xu, K., Ho, K., Kan, H., Fu, Q., Lan, K., 2020. Aerodynamic analysis of SARS-CoV-2 in two Wuhan hospitals. Nature 582, 557–560. https://doi.org/10.1038/s41586-020-2271-3.

Lloyd-Smith, J.O., Schreiber, S.J., Kopp, P.E., Getz, W.M., 2005. Superspreading and the effect of individual variation on disease emergence. Nature 438, 355–359.

Maier, B.F., Brockmann, D., 2020. Effective containment explains subexponential growth in recent confirmed COVID-19 cases in China. Science 368, 742–746. https://doi.org/10.1126/science.abb4557.

Morawska, L., Milton, D., 2020. It is time to address airborne transmission of COVID-19. Clin. Infect. Dis. https://doi.org/10.1093/cid/ciaa939.

Peiris, J.S.M., Yuen, K.Y., Osterhaus, A.D.M.E., Stöhr, K., 2003. The severe acute respiratory syndrome. N. Engl. J. Med. 349, 2431–2441. https://doi.org/10.1056/NEJMra032498.

Prather, K.A., Wang, C.C., Schooley, R.T., 2020. Reducing transmission of SARS-CoV-2. Science 368, 1422–1424. https://doi.org/10.1126/science.abc6197.

Pyankov, O.V., Bodnev, S.A., Pyankova, O.G., Agranovski, I.E., 2018. Survival of aerosolized coronavirus in the ambient air. J. Aerosol Sci. 115, 158–163. https://doi.org/10.1016/j.jaerosci.2017.09.009.

Richard, M., Fouchier, R.A.M., 2016. Influenza A virus transmission via respiratory aerosols or droplets as it relates to pandemic potential. FEMS Microbiol. Rev. 40, 68–85. https://doi.org/10.1093/femsre/fuv039.

Rychlik, K.A., Secrest, J.R., Lau, C., Pulczinski, J., Zamora, M.L., Leal, J., Langley, R., Myatt, L.G., Raju, M., Chang, R.C.-A., Li, Y., Golding, M.C., Rodrigues-Hoffmann, A., Molina, M.J., Zhang, R., Johnson, N.M., 2019. In utero ultrafine particulate matter exposure causes offspring pulmonary immunosuppression. Proc. Natl. Acad. Sci. 116, 3443–3448. https://doi.org/10.1073/pnas.1816103116.

Setti, L., Passarini, F., De Gennaro, G., Barbieri, P., Perrone, M.G., Borelli, M., Palmisani, J., Di Gilio, A., Torboli, V., Fontana, F., Clemente, L., Pallavicini, A., Ruscio, M., Piscitelli, P., Miani, A., 2020. SARS-Cov-2RNA found on particulate matter of Bergamo in northern Italy: first evidence. Environ. Res. 188, 109754. https://doi.org/10.1016/j.envres.2020.109754.

Siegenfeld, A.F., Taleb, N.N., Bar-Yam, Y., 2020. Opinion: what models can and cannot tell us about COVID-19. Proc. Natl. Acad. Sci. U. S. A. 117, 16092–16095. https://doi.org/10.1073/pnas.2011542117.

Stadnytskyi, V., Bax, C.E., Bax, A., Anfinrud, P., 2020. The airborne lifetime of small speech droplets and their potential importance in SARS-CoV-2 transmission. Proc. Natl. Acad. Sci. U. S. A. 117, 11875–11877. https://doi.org/10.1073/pnas.2006874117.

Stutt, R.O.J.H., Retkute, R., Bradley, M., Gilligan, C.A., Colvin, J., 2020. A modelling framework to assess the likely effectiveness of facemasks in combination with 'lockdown' in managing the COVID-19 pandemic. Proc. R. Soc. A Math. Phys. Eng. Sci. 476, 20200376. https://doi.org/10.1098/rspa.2020.0376.

Tang, J.W., Nicolle, A.D., Klettner, C.A., Pantelic, J., Wang, L., Suhaimi, A. Bin, Tan, A.Y.L., Ong, G.W.X., Su, R., Sekhar, C., Cheong, D.D.W., Tham, K.W., 2013. Airflow dynamics of human jets: sneezing and breathing - potential sources of infectious aerosols. PLoS One 8, e59970. https://doi.org/10.1371/journal.pone.0059970.

US Centers for Disease Control and Prevention, 2020. Coronavirus disease 2019 (COVID-19) - social distancing, quarantine, and isolation. https://www.cdc.gov/coronavirus/2019-ncov/prevent-getting-sick/social-distancing.html Accessed 15 July 2020.

Wallace, L.A., Emmerich, S.J., Howard-Reed, C., 2002. Continuous measurements of air change rates in an occupied house for 1 year: the effect of temperature, wind, fans, and windows. J. Expo. Anal. Environ. Epidemiol. 12, 296–306.

Wang, X., Ferro, E.G., Zhou, G., Hashimoto, D., Bhatt, D.L., 2020. Association between universal masking in a health care system and SARS-CoV-2 positivity among health care workers. JAMA https://doi.org/10.1001/jama.2020.12897 Published online July 14, 2020.

World Health Organization, 2020. Coronavirus disease (COVID-2019) situation reports (Geneva, Switzerland). https://www.who.int/emergencies/diseases/novel-coronavirus-2019/situation-reports/ Accessed 15 July 2020.

Wu, G., Brown, J., Zamora, M.L., Miller, A., Satterfield, M.C., Meininger, C.J., Steinhauser, C.B., Johnson, G.A., Burghardt, R.C., Bazer, F.W., Li, Y., Johnson, N.M., Molina, M.J., Zhang, R., 2019. Adverse organogenesis and predisposed long-term metabolic syndrome from prenatal exposure to fine particulate matter. Proc. Natl. Acad. Sci. U. S. A. 116, 11590–11595. https://doi.org/10.1073/pnas.1902925116.

Zhang, R., Wang, G., Guo, S., Zamora, M.L., Ying, Q., Lin, Y., Wang, W., Hu, M., Wang, Y., 2015. Formation of urban fine particulate matter. Chem. Rev. 115, 3803–3855. https://doi.org/10.1021/acs.chemrev.5b00067.

Zhang, R., Li, Y., Zhang, A.L., Wang, Y., Molina, M.J., 2020. Identifying airborne transmission as the dominant route for the spread of COVID-19. Proc. Natl. Acad. Sci. U. S. A. 117, 14857–14863. https://doi.org/10.1073/pnas.2009637117.